Journal of Catalysis 262 (2009) 44–56

Contents lists available at ScienceDirect

Journal of Catalysis

www.elsevier.com/locate/jcat

Evidence for a chromasiloxane ring size effect in Phillips (Cr/SiO_2) polymerization catalysts

Cori A. Demmelmaier [a], Rosemary E. White [a], Jeroen A. van Bokhoven [c], Susannah L. Scott [a,b,*]

[a] Department of Chemical Engineering, University of California, Santa Barbara, CA 93106-5080, USA
[b] Department of Chemistry & Biochemistry, University of California, Santa Barbara, CA 93106-9510, USA
[c] Institute for Chemical and Bioengineering, ETH Zurich, 8093 Zurich, Switzerland

ARTICLE INFO

Article history:
Received 15 September 2008
Revised 23 November 2008
Accepted 24 November 2008
Available online 31 December 2008

Keywords:
Silica
Chromyl chloride
Grafting
Phillips catalyst
Strained siloxane rings
XANES simulation

ABSTRACT

The ambient temperature reaction of CrO_2Cl_2 with silica, followed by mild heating to induce formation of uniform grafted silylchromate diesters, was studied as a function of the silica pretreatment temperature. The reactivity of the resulting chromate sites toward ethylene is qualitatively different: those formed on the silica pretreated at 200 °C are incapable of initiating polymerization, while those formed on silicas pretreated at 450 and 800 °C spontaneously induce polymerization with kinetic profiles closely resembling that of the calcined Phillips catalyst (CrO_x/SiO_2). Comparison of their X-ray absorption spectra suggests subtle differences in the chromate–support interactions, which can be interpreted in terms of changes in the chromasiloxane ring size distribution. The unstrained sites favored on the highly hydroxylated silica surface are consistent with 8-membered chromasiloxane rings formed by attachment of the CrO_2 fragment to non-vicinal hydroxyls, while the strained sites on highly dehydroxylated silica surfaces are suggested to be 6-membered chromasiloxane rings created from vicinal hydroxyls located on adjacent silicon atoms. Simple computational models for these sites predict changes in the vibrational spectra and the XANES that are consistent with experimental observations.

1. Introduction

The Phillips catalyst (CrO_x/SiO_2) is a low-cost, self-activating polymerization catalyst used in 40–50% of the world's annual high-density polyethylene (HDPE) production [1]. The catalyst is made conventionally by wet impregnation of porous silica with aqueous chromate or a chromium(III) salt. Even at low Cr loadings, this method results in incomplete Cr dispersion, manifested as Cr(VI) oligomers and bulk Cr_2O_3 [2], while the dispersed Cr(VI) sites may exhibit both dioxo- and monooxochromium(VI) structures [3]. Non-uniformity is more severe the higher the Cr loading. Polymerization is spontaneously initiated only after the catalyst has been calcined at or above 500 °C [1,4]. Indeed, the catalyst calcination temperature influences, more than any other variable, the behavior of the Phillips catalyst and the properties of the polyethylene it produces [1,5]. Maximum activity is obtained at a loading of ca. 0.4 Cr/nm^2 (typically, 1 wt% Cr) [6] and when the catalyst is heated at 925 °C, just prior to sintering of the support [1]. However, since anchoring of chromium to the silica surface as the silylchromate diester is complete at much lower temperatures (350 °C), the activation of the catalyst may involve another, as yet unknown, thermal transformation [5].

While ethylene reduces Cr(VI), not all reduced sites become active centers [7]. Typically, only 1–10% of the Cr sites are activated upon exposure to ethylene [4]. The precise nature of the first Cr–C bond-forming reaction, as well as structural details of the active sites, remains a mystery. Unfortunately, the sites present on catalysts with the lowest Cr loadings are both the most relevant and the most challenging to study spectroscopically. Greater active site uniformity would therefore facilitate mechanistic studies. It would also lead to more efficient activation, thereby decreasing the amount of catalyst residue in the polymer [8–10]. Finally, it should result in improved control over polymer microstructure, for example, the distribution of polyethylene molecular weights, and short- and long-chain branching [1,4].

We [11] and others [12,13] have postulated that silica-supported chromium catalysts prepared via CrO_2Cl_2 grafting should have more uniform sites, and consequently be more active [4,14], than those prepared by the traditional impregnation method. Volatile CrO_2Cl_2 is reported to react with various oxide surfaces to produce highly dispersed monochromate sites [4,15–18]. In these materials, as in the Phillips catalyst, the presence of residual chloride is generally detrimental; strategies to ensure its complete removal include codeposition or alternating deposition with a reactive gas

* Corresponding author.
E-mail address: sscott@engineering.ucsb.edu (S.L. Scott).

0021-9517/$ – see front matter
doi:10.1016/j.jcat.2008.11.024

such as H_2 or water vapor [19–21]. However, the presence or formation of water can lead to aggregation of chromium oxides. Recently, we reported on the room temperature interaction between CrO_2Cl_2 vapor and silica surfaces under anhydrous conditions [11]. On silicas pretreated at 200 and 450 °C, only $\equiv SiOCrO_2Cl$ sites are formed, despite the presence of unreacted silanols. The reactivity of some silanols may be diminished by hydrogen-bonding interactions with adjacent grafted monochlorosilylchromate monoester sites, Eq. (1).

$$2{\equiv}SiOH + CrO_2Cl_2 \rightarrow {\equiv}SiOCrO_2Cl...HOSi{\equiv} + HCl \quad (1)$$

These monoester sites are unreactive toward ethylene [11], presumably due to the presence of the remaining chloride ligand.

On silica pretreated at 800 °C and exposed to CrO_2Cl_2 at room temperature, we found that, in addition to $\equiv SiOCrO_2Cl$, a minor amount of chromate diester is produced directly [11]. Since the latter is not formed via a concerted reaction of CrO_2Cl_2 with silanol pairs on more hydroxylated silica surfaces, we suggested that it arises by the interaction of CrO_2Cl_2 with a highly strained siloxane ring. Such rings are created at 800 °C via the condensation of a pair of vicinal silanols [22,23]. This condensation is more facile when one silanol is also a member of a geminal pair, Eq. (2), since only three links are required between the four-membered siloxane ring and the silica lattice (compared to four in the case of rings formed by condensation between pairs of vicinal silanols, neither of which is geminal) [24]. The reaction of CrO_2Cl_2 with such hydroxyl-bearing siloxane rings to give chromate diester sites via transfer of a chloride ligand to silicon was calculated to be exothermic, Eq. (3) [11]. However, these sites also proved unable to initiate ethylene polymerization.

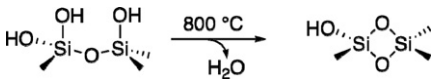

(2)

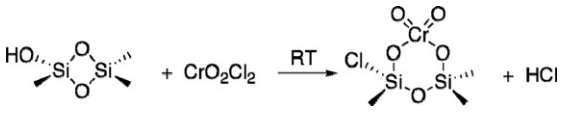

(3)

The anchoring of chromate sites on silica necessarily involves formation of chromasiloxane rings. The ring size is determined by the disposition of the original pair of silanols (represented as $2{\equiv}SiOH$ in Eq. (1)) that serve to attach each chromate fragment to the silica surface. The relationships between pairs of silanols are, in turn, a function of the catalyst calcination temperature (in the case of wet impregnation) or the silica pretreatment temperature (in the case of anhydrous grafting). Obtaining structural information about the chromasiloxane rings formed on amorphous silica is complicated by their non-uniformity. Uniform chromates have been prepared at high site densities on planar silica surfaces [25], although their low absolute numbers make characterization challenging [7]. All of these materials are extremely air-sensitive, necessitating scrupulously clean handling at every stage of catalyst processing.

In this contribution, we attempt to probe the various chromasiloxane rings formed on CrO_2Cl_2-modified silicas and their dependence on the silica pretreatment temperature, using a combination of IR, XANES and EXAFS spectroscopies, as well as DFT computational modeling of the grafted sites. We also investigate the relationship between chromate sites prepared by our anhydrous grafting method and the initiating sites of a standard Phillips catalyst. A link between the catalyst activation temperature, the average chromasiloxane ring size, and polymerization activity is proposed.

2. Experimental and computational methods

2.1. Sample preparation

The silica used in this study is Sylopol 952, a silica gel from Grace-Davison with a surface area of ca. 310 m^2/g, a pore volume of 1.61 mL/g and an average particle size of 112 μm. It is found in commercial formulations of the Phillips (Cr/SiO_2) ethylene polymerization catalyst. The silica was pretreated by heating to the desired temperature (200, 450, or 800 °C) under dynamic vacuum ($<10^{-4}$ Torr) on a liquid N_2-trapped high vacuum line for a minimum of 4 h. The surface area does not change significantly as a result of this thermal treatment. The silicas are labeled S952-X, where X denotes the silica pretreatment temperature in °C. After thermal treatment, each sample was handled either under vacuum or in an inert atmosphere at all times, to prevent readsorption of atmospheric moisture.

CrO_2Cl_2-modified silicas were prepared by grafting CrO_2Cl_2 vapor (99.99+%, Aldrich) under reduced pressure at room temperature onto dehydrated and partially dehydroxylated Sylopol 952 to yield an orange powder, as described previously [11]. After evacuation of volatiles, the modified silicas were heated at 200 °C under dynamic vacuum for a minimum of two hours, to effect the quantitative transformation of grafted $\equiv SiOCrO_2Cl$ sites to $(\equiv SiO)_2CrO_2$ (vide infra). Standard Phillips catalysts were prepared by stirring an aqueous solution of CrO_3 solution in deionized water with Sylopol 952 until the water evaporated, giving an orange powder. These materials were heated slowly to 800 °C either *in vacuo* or under O_2, as specified, then calcined at 800 °C in oxygen for a minimum of four hours. These catalysts generally retained their orange color; samples that turned green were discarded.

The reference compounds $[CrO_2\{(OSiPh_2)O\}]_2$ and $CrO_2(OSiPh_3)_2$ were synthesized according to published procedures [26,27].

2.2. Characterization

Elemental analysis (Cr, Cl) was conducted as previously described [11]. An in situ cell for infrared spectroscopy under controlled atmosphere was used to record spectra of the air-sensitive catalysts. The procedure for acquisition of X-ray absorption spectra has been described [11]. Precise energy calibration was ensured by recording the transmission spectrum of a Cr calibration foil (K-edge 5989.0 eV) [28] simultaneously with the fluorescence spectrum of each sample. A reference spectrum of Cr_2O_3 for linear combination analysis was obtained from the XAFS Model Compound Library [29].

2.3. Polymerization kinetics

Ethylene (Praxair, 5.0 grade) was passed through a column containing activated BTS catalyst (Aldrich) and molecular sieves (4 Å, Aldrich) to remove traces of O_2 and water, respectively, and was stored in a dry glass bulb containing activated molecular sieves. Approximately 600 Torr ethylene was expanded from the storage bulb into a preheated reaction flask (ca. 90 mL, 120 ± 5 °C). The kinetics of ethylene uptake by the catalysts were monitored by recording the pressure at timed intervals during the reaction, using a 750B Baratron High Pressure Absolute Pressure Transducer (MKS Instruments, 750B13TCD2GA, range 0.1–1000 Torr).

2.4. Computational methods

Geometry optimizations, reaction enthalpies and frequency calculations for model clusters were performed using DFT, as previously described [11]. To simulate the XANES of model clusters,

ab initio real-space, full multiple-scattering calculations were performed using the FEFF 8.20 code [30]. It implements self-consistent field potentials for the determination of the Fermi level and the extent of charge transfer. Calculations were performed using the Hedin–Lundquist exchange correlation potential. A core-hole was included on the absorber atom to mimic the final state of the photon absorption process.

3. Results

3.1. Thermal treatment of CrO_2Cl_2-modified silicas

When S952 silica is pretreated at either 200 or 450 °C, then exposed to excess CrO_2Cl_2, evolution of HCl is observed. The HCl was identified by in situ gas phase IR spectroscopy via its characteristic rovibrational manifold centered at 2900 cm^{-1}. The reaction yields primarily $\equiv SiOCrO_2Cl$ via simple protonolysis of CrO_2Cl_2 by some (not all) of the surface hydroxyl groups [11]. When the yellow-orange Cr-modified silicas were heated at 200 °C under dynamic vacuum for at least two hours, more HCl was liberated and the materials became lighter in color. Heating also results in loss of CrO_2Cl_2; it was collected as an orange-red liquid in a liquid-N_2 cold trap.

The formation of HCl implies a reaction between $\equiv SiOCrO_2Cl$ sites and residual silanol groups, the latter presumably located immediately adjacent to the grafted sites, as in Eq. (1). However, HCl may diffuse away from its site of origin to encounter non-adjacent $\equiv SiOCrO_2Cl$ sites. Their subsequent reaction could liberate CrO_2Cl_2 according to Eq. (4), thereby accounting for its observed release from the silica. Alternatively, CrO_2Cl_2 may be formed by a reaction between two adjacent grafted $\equiv SiOCrO_2Cl$ sites, Eq. (5).

$$\equiv SiOCrO_2Cl + HCl \rightarrow \equiv SiOH + CrO_2Cl_2 \quad (4)$$

$$2\equiv SiOCrO_2Cl \rightarrow (\equiv SiO)_2CrO_2 + CrO_2Cl_2 \quad (5)$$

After heating for two hours, the Cr content of CrO_2Cl_2-modified S952-200 declined almost negligibly, from 1.53 to 1.49 wt% (i.e., from 0.294 to 0.287 mmol Cr/g), although a small amount of CrO_2Cl_2 was detected visually. For CrO_2Cl_2-modified S952-450, a larger decline was recorded, from 0.66 to 0.50 wt% (i.e., from 0.127 to 0.096 mmol Cr/g). Simultaneously, the chloride content of both silicas decreased to <0.03 wt% (<0.001 mmol/g), which is below the detection limit. This result implies virtually quantitative transformation of the $\equiv SiOCrO_2Cl$ sites to $(\equiv SiO)_2CrO_2$.

When S952-800 is exposed to CrO_2Cl_2 at room temperature, the majority of the grafted chromium sites are still described as $\equiv SiOCrO_2Cl$, however, $(\equiv SiO)_2CrO_2$ sites are also formed (ca. one-third of the total), by opening of the strained siloxane 2-ring as shown in Eq. (3) [11]. The measured Cr/Cl ratio of 1.0 for this material is consistent with siloxane ring-opening accompanied by transfer of a chloride ligand to silicon ($\equiv SiCl$). Some surface hydroxyl groups of S952-800 persist even in the presence of excess CrO_2Cl_2 and after addition of several doses of the volatile reagent. We also heated this CrO_2Cl_2-modified silica at 200 °C under dynamic vacuum for two hours. Its Cr content declined only slightly, from 0.30 to 0.25 wt%, and its chloride content decreased by a corresponding amount. This result is consistent with a minor reaction of adjacent grafted $\equiv SiOCrO_2Cl$ sites to form $(\equiv SiO)_2CrO_2$, according to Eq. (5).

3.2. Ethylene polymerization activity

The ability of each of the chromyl chloride-modified silicas to initiate ethylene polymerization was evaluated in a batch reactor at 120 °C, after first being heated *in vacuo* at 200 °C to effect the transformation of $\equiv SiOCrO_2Cl$ sites to chromates, $(\equiv SiO)_2CrO_2$.

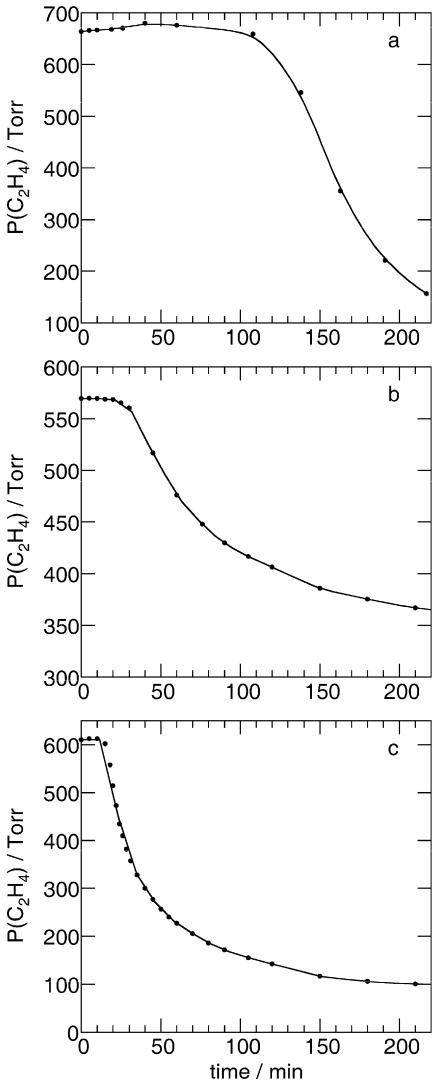

Fig. 1. Ethylene uptake profiles in a batch reactor at (120 ± 5) °C, over (a) 72.5 mg CrO_2Cl_2-modified S952-450 (0.23 wt% Cr, 3.2 μmol Cr); (b) 32.9 mg CrO_2Cl_2-modified S952-800 (0.26 wt% Cr, 1.6 μmol Cr); both recorded after heating the modified silica *in vacuo* at 200 °C; and (c) 25.2 mg Phillips catalyst (0.66 wt% Cr, 3.2 μmol Cr), calcined at 800 °C. Lines are drawn only as a guide to the eye.

None of the chromyl chloride-modified silicas showed any reactivity toward ethylene prior to this thermal treatment, therefore neither $\equiv SiOCrO_2Cl$ sites nor the minor chromate sites formed spontaneously from CrO_2Cl_2 on S952-800 activate. However, after elimination of the chloride ligand, the chromate sites present on S952-450 initiated ethylene polymerization following a prolonged induction period (>100 min; 3.2 μmol Cr), Fig. 1. In contrast, the chloride-free chromate sites prepared on S952-200 were completely inactive. A standard Phillips catalyst containing the same amount of Cr (3.2 μmol) was tested under the same reaction conditions. It exhibited rapid ethylene uptake following a short induction period (15 min).

The activity of these catalysts is difficult to quantify because of the batch nature of the reaction (i.e., $P(C_2H_4)$ changes with time), and the slow activation of sites in comparison to propagation (i.e., the number of active sites changes with time). In addition, the extreme sensitivity of these scavenger-free catalysts to impurities adds considerable uncertainty to the measured rates and induction periods. Nevertheless, the difference in the activity of the catalysts made by grafting CrO_2Cl_2 onto S952-450 and S952-800 is real and reproducible. After thermal treatment at 200 °C, chromate

sites made from $\equiv SiOCrO_2Cl$ on S952-800 (1.6 μmol Cr) show a much shorter induction period, ca. 30 min, compared to those on S952-450. We therefore sought to probe the differences between chromates that lead to active and inactive polymerization sites on each of our "well-defined" grafted catalysts.

3.3. DFT modeling of chromate sites embedded in siloxane rings

The formation of $(\equiv SiO)_2CrO_2$ sites from $\equiv SiOCrO_2Cl$ was explored computationally, using siloxane oligomers with mixed hydrogen- and hydroxyl-termination to represent the silica support and chromasiloxane rings to represent the silylchromate diesters. Elimination of HCl from the internally hydrogen-bonded monochlorosilylchromate monoester **I**, located adjacent to a non-vicinal silanol, to form the cyclic silylchromate diester **II** as part of an 8-membered chromasiloxane ring is mildly endothermic, Scheme 1. This reaction models the formation of large, unstrained chromasiloxane rings which are the expected mode of chromate anchoring on fully hydroxylated silica surfaces, such as S952-200 [24]. On such silicas, thermal dehydroxylation has been shown to lead predominantly to siloxane 3-rings, indicating that the condensing hydroxyl groups are separated by three (SiO) units [31]. Elimination of CrO_2Cl_2 from adjacent, non-vicinal monochlorosilylchromate monoester sites in **III** to form the cyclic chromate **II** has a similar reaction enthalpy. Thus both reactions appear to be feasible upon mild heating of CrO_2Cl_2-modified S952-200.

The calculated bond distances d(Cr=O), 1.560 and 1.567 Å, in **II** are similar to those found in the molecular chromates $CrO_2(OSiPh_3)_2$ and $[CrO_2\{(OSiPh_2)_2\}]_2$, 1.514–1.579 Å; the calculated bond distance d(Cr–O), 1.742 Å, also compares well to 1.706–1.782 Å in the molecular compounds [26,27], Table 1. The Cr environment in **II** is very close to tetrahedral. The internal ring angles in the 8-membered chromasiloxane ring are 130 and 147° for CrOSi and SiOSi, respectively. For comparison, the angles in the 8-membered ring of a silsesquioxane chromate are 135.4 and 135.2° (CrOSi) and 145–149° (SiOSi) [32]. In particular, the SiOSi angle in **II** suggests a fairly low-strain ring, since amorphous silicas have SiOSi angles in the range 147–151° [33]. The ring closure **I** → **II** causes a very slight increase in the calculated $\nu_a(CrO_2)$ frequency (from 998 to 1000 cm^{-1}), and a larger decrease in the calculated $\nu_s(CrO_2)$ frequency (from 987 to 970 cm^{-1}), Table 2.

Weakly interacting or non-interacting vicinal silanols dominate the surfaces of silicas pretreated at temperatures in excess of 400 °C [34]; their persistence is attributed to the highly un-

Table 1
Selected distances (Å) and angles (°) for calculated structures of model chromasiloxane rings.

Model	Distances		Angles	
II	Cr=O	1.560, 1.567	O=Cr=O	110.4
	Cr–O	1.742	O–Cr–O	109.4
	Si–O(Cr)	1.671	O=Cr–O	108.3, 110.2
	Si–O(Si)	1.636, 1.644	Cr–O–Si	130.1, 130.0
	Cr–Si	3.095, 4.104	Si–O–Si	146.9, 146.6
V	Cr=O	1.559, 1.566	O=Cr=O	110.3
	Cr–O	1.748	O–Cr–O	104.2
	Si–O(Cr)	1.676, 1.674	O=Cr–O	109.2, 111.9
	Si–O(Si)	1.649, 1.648	Cr–O–Si	123.1, 123.4
	Cr–Si	3.011, 3.013	Si–O–Si	135.2

Table 2
Calculated fundamental frequencies (cm^{-1}) for computational model structures and observed IR overtone frequencies (cm^{-1}) for silylchromate esters on various silicas.

Model compounds		$\nu_a(CrO_2)$	$\nu_s(CrO_2)$
$CrO_2Cl[(OSiH_2)_3OH]$, **I**		998	987
$CrO_2[H_2SiO(H_2SiO)_2]$, **II**		1000	970
$CrO_2Cl[(OSiH_2)_2OH]$, **IV**		1000	991
$CrO_2[O(H_2SiO)_2]$, **V**		1005	975
$CrO_2Cl[OSiH(OSiH_2)_2O]$, **XII**		997	986
$CrO_2[OSiCl(H)(OSiH_2)_2O]$, **XIII**		1002	973
Silylchromate diesters[a]	$2\nu_a(CrO_2)$	$\nu_a(CrO_2)+\nu_s(CrO_2)$	$2\nu_s(CrO_2)$
on S952-200:	2001	1980	1964
on S952-450: $\equiv SiOCrO_2Cl$	1999	1979	1967
on S952-800: $\equiv SiOCrO_2Cl$	2000	1981	1971
Phillips catalyst[b]	2003	1983	1970

[a] Prepared by grafting CrO_2Cl_2 on silica pretreated at the specified temperature, followed by heating under dynamic vacuum at 200 °C for 2 h.

[b] Prepared by wet impregnation of S952 silica with CrO_3 (0.5 wt% Cr), followed by drying and slow heating in vacuum to 800 °C, then calcination in O_2 at 800 °C.

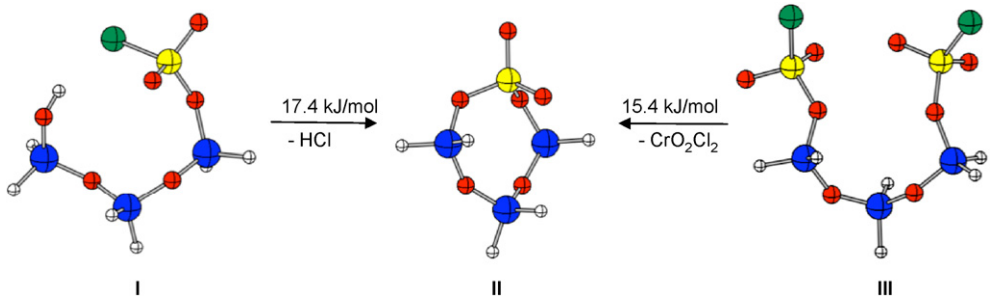

Scheme 1. Computational model for a grafted $(\equiv SiO)_2CrO_2$ site as part of an 8-membered chromasiloxane ring (**II**), and its enthalpy of formation from $\equiv SiOCrO_2Cl$ sites via elimination of HCl by reaction with a non-vicinal silanol (**I**), or via elimination of CrO_2Cl_2 by reaction with a non-vicinal $\equiv SiOCrO_2Cl$ site (**III**). Color key: Cr (yellow), Cl (green), O (red), Si (blue), H (white). (For interpretation of the references to color in this figure legend, the reader is referred to the web version of this article.)

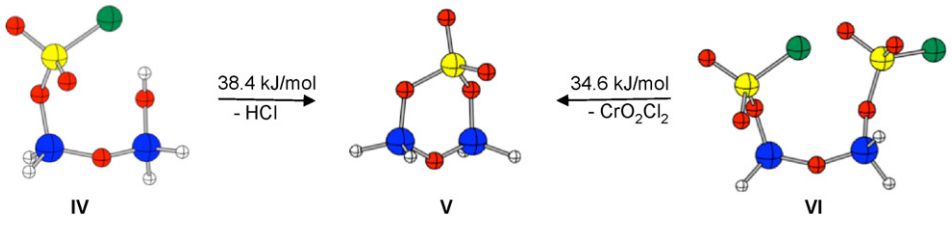

Scheme 2. Computational model for a grafted $(\equiv SiO)_2CrO_2$ site containing a 6-membered chromasiloxane ring (**V**), and its enthalpy of formation from $\equiv SiOCrO_2Cl$ via elimination of HCl by reaction with a vicinal silanol (**IV**), or by elimination of CrO_2Cl_2 via reaction with a vicinal $\equiv SiOCrO_2Cl$ site (**VI**). Color key: Cr (yellow), Cl (green), O (red), Si (blue), H (white). (For interpretation of the references to color in this figure legend, the reader is referred to the web version of this article.)

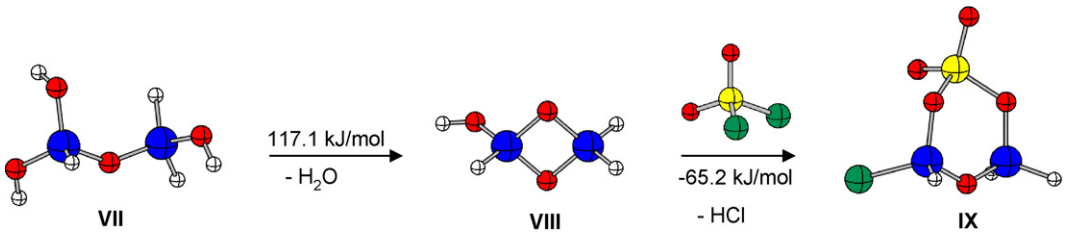

Scheme 3. Computational model for spontaneous formation of the cyclic silylchromate diester **IX** by reaction of CrO_2Cl_2 with the hydroxyl-substituted siloxane 2-ring **VIII** (from condensation within the vicinal–geminal silanol pair **VII**). Color key: Cr (yellow), Cl (green), O (red), Si (blue), H (white). (For interpretation of the references to color in this figure legend, the reader is referred to the web version of this article.)

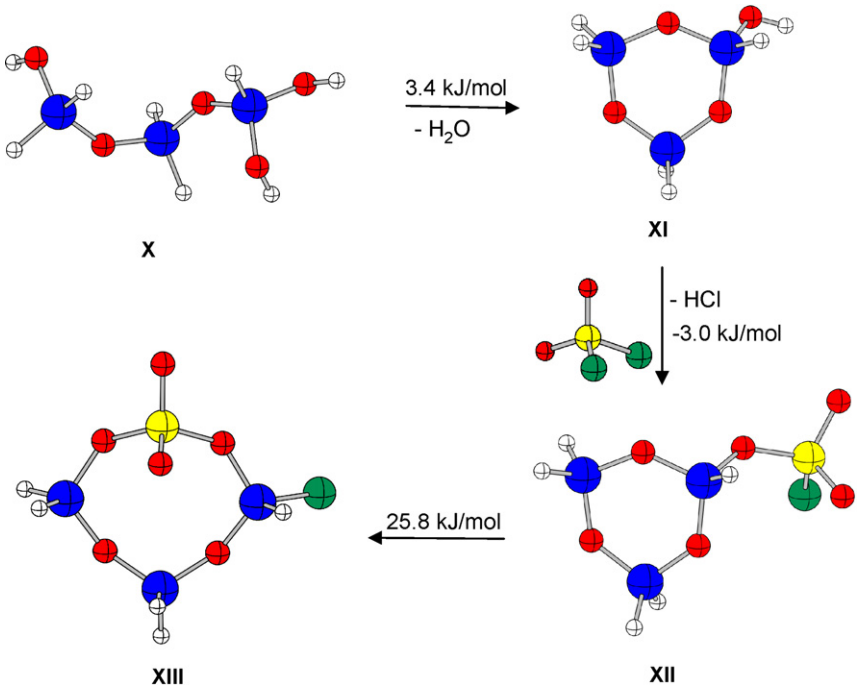

Scheme 4. Computational model for the thermal conversion of grafted $\equiv SiOCrO_2Cl$ to $(\equiv SiO)_2CrO_2$ on S952-800, without loss of chloride. Color key: Cr (yellow), Cl (green), O (red), Si (blue), H (white). (For interpretation of the references to color in this figure legend, the reader is referred to the web version of this article.)

favorable mutual condensation to give strained four-membered siloxane rings [35]. Scheme 2 shows the elimination of HCl from monochlorosilylchromate monoester **IV**, located vicinal to a silanol, to give the silylchromate diester **V** as part of a 6-membered chromasiloxane ring. This reaction is more endothermic than the transformation of **I** to **II**, although it still appears to be feasible with mild heating. Elimination of CrO_2Cl_2 from the vicinal bis(chlorochromate) structure **VI** to form **V** is uphill by a similar amount. The distances d(Cr=O) and d(Cr–O) are virtually the same in both **II** and **V**, however, greater strain in the 6-membered chromasiloxane ring relative to the 8-membered ring **II** is indicated by the smaller CrOSi and SiOSi angles, 123 and 135°, respectively, as well as the smaller O=Cr–O angle, 104.2° (compared to 109.4° for **II**), Table 1. Small shifts in the frequencies of the calculated $\nu(CrO_2)$ modes upon transformation of **IV** to **V** are very similar to those predicted for the formation of the larger ring. Thus we find (as have others [36,37]) that O=Cr=O bond lengths, angles and stretching frequencies are rather insensitive to chromasiloxane ring size/strain, Tables 1–2.

In Schemes 1–2, the chlorochromate to chromate transformation is achieved by loss of chloride, consistent with our observation of low residual chloride after thermolysis of CrO_2Cl_2-modified S952-200 and -450. However, the chloride content of CrO_2Cl_2-modified S952-800 does not decline much when this material is heated, although IR and XAS evidence suggests that the remaining chloride is not bound to Cr (see below). Therefore we explored possible reactions involving chloride transfer from Cr to Si. One such reaction was previously proposed for the direct formation of chromate sites during room temperature-grafting of CrO_2Cl_2 on highly dehydroxylated silica [11]. It is based on the appearance of highly strained siloxane 2-rings upon heating silica to 800 °C [22,38]. The 2-rings formed at the lowest temperatures arise by condensation of a vicinal silanol pair where one of the silanols is also a member of a geminal pair [24], as in **VII**, Scheme 3. The reaction of the strained 2-ring **VIII** with CrO_2Cl_2 to give the chromasiloxane ring **IX** is indeed exothermic, by 65 kJ/mol. The calculated frequencies of the $\nu(CrO_2)$ modes closely resemble those of **V**.

Although rings such as **IX** were proposed to account for up to one-third of the supported Cr(VI) sites on S952-800 [11], the majority of the sites (two-thirds of all anchored Cr) were identified as $\equiv SiOCrO_2Cl$ by XANES and EXAFS, and are presumably formed by reaction with the remaining surface silanols. Scheme 4 shows a possible mechanism for their formation. At temperatures above 400 °C, condensation of non-vicinal silanols where one silanol is a member of a geminal pair (**X**) leads to the formation of a siloxane 3-ring bearing a silanol group, **XI**. Reaction of the remaining silanol with CrO_2Cl_2 is close to thermoneutral, and results in the formation of **XII**, bearing a chlorochromate substituent. Upon mild heating, rearrangement of this substituted 3-ring to the larger ring **XIII** may occur by transfer of chlorine from Cr to Si. This reaction

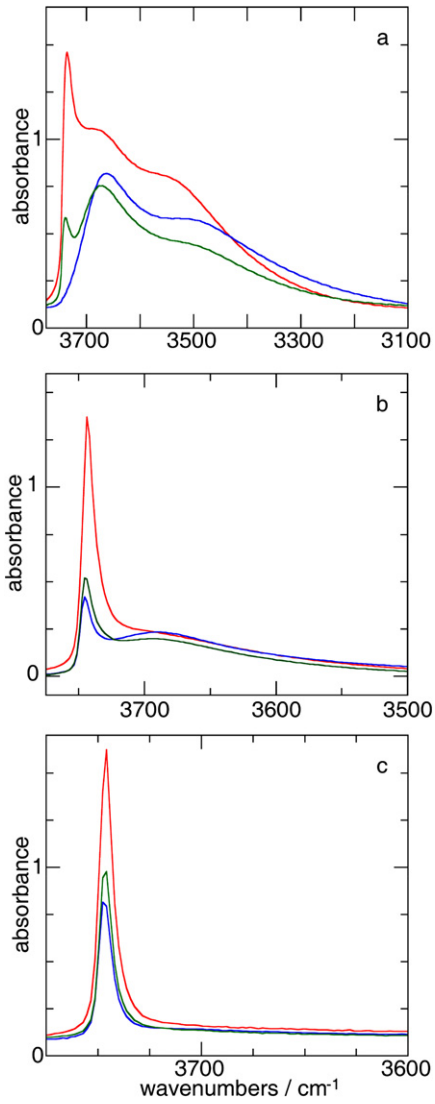

Fig. 2. Transmission IR spectra in the ν(OH) region, for (a) S952-200; (b) S952-450; and (c) S952-800 (red lines); as well as for each sample after grafting CrO_2Cl_2 at room temperature (blue lines), and after heating each of the CrO_2Cl_2-modified silicas *in vacuo* at 200 °C (green lines). All spectra were baseline-corrected and normalized to the intensity of the silica lattice overtone at 1870 cm^{-1}. (For interpretation of the references to color in this figure legend, the reader is referred to the web version of this article.)

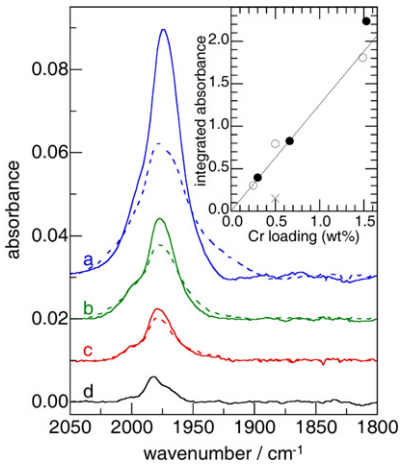

Fig. 3. Comparisons of difference IR spectra, for CrO_2Cl_2 grafted onto (a) S952-200; (b) S952-450; and (c) S952-800; both before (solid lines) and after (dashed lines) heating to 200 °C under dynamic vacuum; and (d) for CrO_3 supported on Sylopol 952 and calcined at 800 °C (Phillips catalyst, 0.50 wt% Cr). The transmission spectra were first normalized using the intensity of the silica lattice overtone at 1870 cm^{-1}, then the difference spectra were obtained by subtracting the appropriately pretreated silica spectrum. Spectra are vertically offset for clarity. The inset shows the integrated absorbance for the region 2050–1900 cm^{-1} as a function of Cr loading for each type of CrO_2Cl_2-modified silica, before (filled circles) and after heating at 200 °C (open circles), as well as for the calcined Phillips catalyst (×).

is predicted to be only slightly endothermic. Shifts in the frequencies of the calculated $\nu(CrO_2)$ modes upon transformation of **XII** to **XIII** are similar to those predicted for the conversion of **I** to **II**, Table 2.

3.4. Infrared spectroscopy

For each type of CrO_2Cl_2-modified S952, heating *in vacuo* at 200 °C causes subtle changes in the ν(OH) region of the IR spectrum. For S952-200, the intensity of the broad peak centered at ca. 3500 cm^{-1} attributed to silanols perturbed by hydrogen-bonding decreases, Fig. 2a. This is consistent with some of the $\equiv SiOCrO_2Cl$ sites reacting with residual silanol sites $\equiv SiOH$ to liberate HCl, Eq. (1). At the same time, the peak at 3740 cm^{-1} assigned to non-interacting or weakly hydrogen-bonded silanols reappears. This observation is consistent with Eq. (4), in which some of the HCl liberates CrO_2Cl_2 from other $\equiv SiOCrO_2Cl$ sites, regenerating free $\equiv SiOH$. Similar changes were observed for CrO_2Cl_2-modified S952-450, Fig. 2b. Although no hydrogen-bonded silanols are evident in the IR spectrum of CrO_2Cl_2-modified S952-800, Fig. 2c, the intensity of the ν(OH) mode of the non-hydrogen-bonded silanols at 3746 cm^{-1} increases slightly upon heating.

The $\nu(CrO_2)$ fundamentals of the $\equiv SiOCrO_2Cl$ and $(\equiv SiO)_2CrO_2$ sites are masked by intense absorption due to silica lattice vibrations in the region near 1000 cm^{-1}, however, their first overtones and combination bands are readily detected by spectral subtraction, Fig. 3. The normalized intensities decrease with increasing silica pretreatment temperature because CrO_2Cl_2 uptake depends on the hydroxyl content of the silica. By analogy to the gas phase IR spectra of CrO_2X_2 (X = F, Cl) [39], these features are assigned to the modes $2\nu_a(CrO_2)$, $\nu_a(CrO_2) + \nu_s(CrO_2)$ and $2\nu_a(CrO_2)$. Peak maxima obtained by spectral deconvolution show little dependence on the silica pretreatment temperature. However, they agree in general with the frequencies predicted for the corresponding fundamentals of the DFT cluster models in Table 2.

Upon heating the CrO_2Cl_2-modified silicas at 200 °C under vacuum, the bands in the overtone region broaden, particularly on the low energy side, while their overall intensities decrease, consistent with some loss of CrO_2Cl_2 from the surface (Eqs. (4)–(5)). In each case, the integrated absorbance is consistent with the expected Cr content for each type of CrO_2Cl_2-modified silica (Fig. 3, inset). The broadening is consistent with the increase in $\nu_a(CrO_2)$ and decrease in $\nu_s(CrO_2)$ predicted by DFT upon forming the model diester clusters from the corresponding monoesters. The position of the deconvoluted peak at ca. 1965 cm^{-1} assigned to $2\nu_s(CrO_2)$ is consistent with the observation of this overtone at 1960 cm^{-1} in a resonance Raman study of 3% CrO_3/SiO_2 calcined at 500 °C [40]. Its blue-shift with increasing silica pretreatment temperature (from 1964 to 1967 to 1971 cm^{-1} for chromates on silicas heated at 200, 450 and 800 °C, respectively) mirrors the small increase in the frequency of the $\nu_s(CrO_2)$ mode for the Raman spectra of 1 wt% Cr/SiO_2 with increasing calcination temperature [36]. The band at ca. 2000 cm^{-1} is consistent with the contribution of the $\nu_a(CrO_2)$ fundamental to a band at 1004 cm^{-1} [36,41], making the most likely assignment of the most intense band at ca. 1980 cm^{-1} the combination mode $\nu_a(CrO_2) + \nu_s(CrO_2)$. Although the appearance of these spectra is similar to that for a standard Phillips catalyst heated under vacuum then calcined in O_2 at 800 °C, Fig. 3d, the latter has a much lower integrated intensity relative to its Cr load-

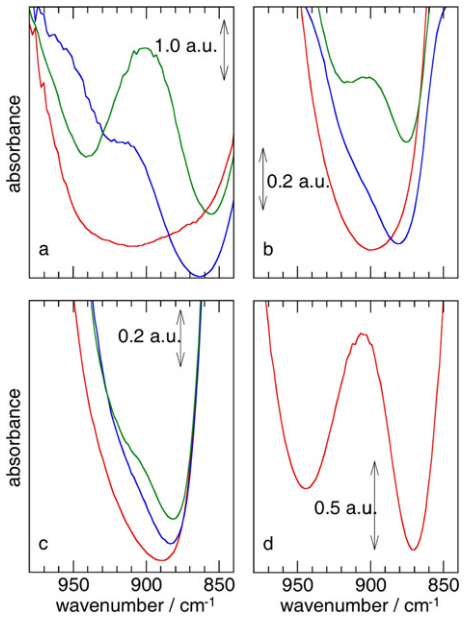

Fig. 4. Transmission IR spectra of silicas (red): (a) S952-200; (b) S952-450; and (c) S952-800; followed by the reaction of each silica with CrO_2Cl_2 (blue) and heating of the Cr-modified silicas at 200 °C under vacuum (green); (d) CrO_3 on Sylopol 952 (Phillips catalyst, 0.50 wt% Cr), after calcination at 800 °C. (For interpretation of the references to color in this figure legend, the reader is referred to the web version of this article.)

ing, suggesting that a significant amount of Cr may not be present as the simple silylchromate diester [2].

The IR spectrum of the Phillips catalyst also contains an intense peak at 905 cm^{-1}, located in the partially transparent "window" region of the silica spectrum below 1000 cm^{-1}, Fig. 4. It has been assigned to a ν(CrO–Si) vibration of a grafted silylchromate diester site [3,41,42]. The spectra of each of the CrO_2Cl_2-modified silicas display a shoulder at ca. 915 cm^{-1}, which increases in intensity and shifts to 900 cm^{-1} upon heating to 200 °C. A comparison of the relative intensities of this peak in Figs. 4a–4c with that in Fig. 4d suggests that species other than the silylchromate diester are at least partly responsible for this feature in the spectrum of the Phillips catalyst.

3.5. XANES analysis

The normalized Cr K-edge XANES spectra of CrO_2Cl_2 grafted onto S952-200, S952-450 and S952-800 are shown in Fig. 5, both before and after heating at 200 °C. All of the K-edges are shifted by ca. 17 eV relative to the Cr foil spectrum, consistent with the K-edge energies of known Cr(VI) compounds [43], including the molecular silylchromate diesters $CrO_2(OSiPh_3)_2$ and $[CrO_2\{(OSiPh_2)_2O\}]_2$. Each of the XANES spectra feature a shoulder at 6.008 keV, superimposed on the main absorption edge. It is associated with the presence of the Cl ligand [11]. For each of the silicas, this feature decreases in intensity upon heating, implying displacement of the Cl ligand and formation of $(\equiv SiO)_2CrO_2$ sites. This is true even for CrO_2Cl_2-modified S952-800, whose total chloride content declines little upon thermal treatment. The K-edge positions do not change significantly upon heating, confirming that the oxidation state Cr(VI) remains unchanged.

Each of the XANES spectra of the CrO_2Cl_2-modified silicas contains a prominent pre-edge peak at 5.998 keV [44,45], attributed to a combination of quadrupolar $1s \rightarrow 3d$ and dipolar $1s \rightarrow 4p$ transitions in a pseudo-tetrahedral (e.g., C_{2v}) environment [46,47]. Its normalized intensity is virtually identical (0.70 ± 0.02) in all of the spectra, indicating that the symmetry at Cr is the same for all of the $\equiv SiOCrO_2Cl$ sites. However, the behavior of the pre-edge

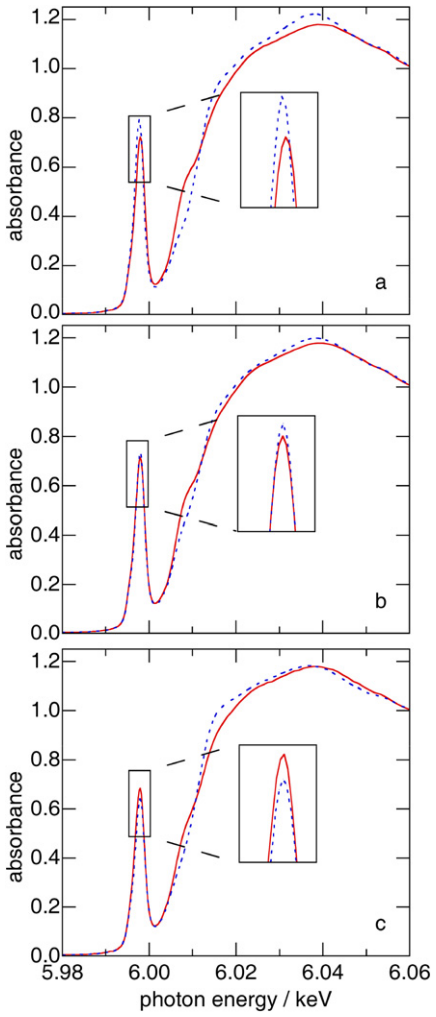

Fig. 5. Normalized Cr K-edge XANES spectra of CrO_2Cl_2-modified (a) S952-200; (b) S952-450; and (c) S952-800; before (red solid line) and after (blue dashed line) heating at 200 °C under vacuum. (For interpretation of the references to color in this figure legend, the reader is referred to the web version of this article.)

peak depends on the silica pretreatment temperature. For S952-200, conversion of $\equiv SiOCrO_2Cl$ to $(\equiv SiO)_2CrO_2$ causes the pre-edge peak to increase in intensity, Fig. 5a, consistent with an increase in local symmetry upon loss of the chloride ligand. For S952-800, the pre-edge peak decreases in intensity during the same transformation, Fig. 5c. Consequently, we infer that the $(\equiv SiO)_2CrO_2$ site on this silica is significantly distorted from C_{2v} symmetry. On S952-450, the pre-edge intensity after heating is virtually unchanged, Fig. 5b, suggesting a cancellation of two opposing effects. The normalized intensities of the pre-edge peaks are 0.79, 0.72 and 0.64 for the chromate sites on S952-200, -450 and -800, respectively.

The XANES spectra of the silylchromate diesters derived from chromyl chloride-modified silicas also show increased intensity at 6.016 and 6.038 keV. The former is more pronounced for S952-800, while the latter is more pronounced for S952-200, as shown in Figs. 6a and 6b. Although small, these features were reproduced in three independent experiments, for which precise energy calibration was assured by simultaneously collecting fluorescence data (for the sample) and transmission data (for a Cr foil reference located behind the sample). To understand the origin of these differences, we examined the XANES of the two molecular silylchromate diesters. The feature at 6.016 keV is slightly more intense for acyclic $CrO_2(OSiPh_3)_2$, while the feature at 6.038 keV is slightly more pronounced for cyclic $[CrO_2\{(OSiPh_2)_2O\}]_2$, Figs. 6c and 6d.

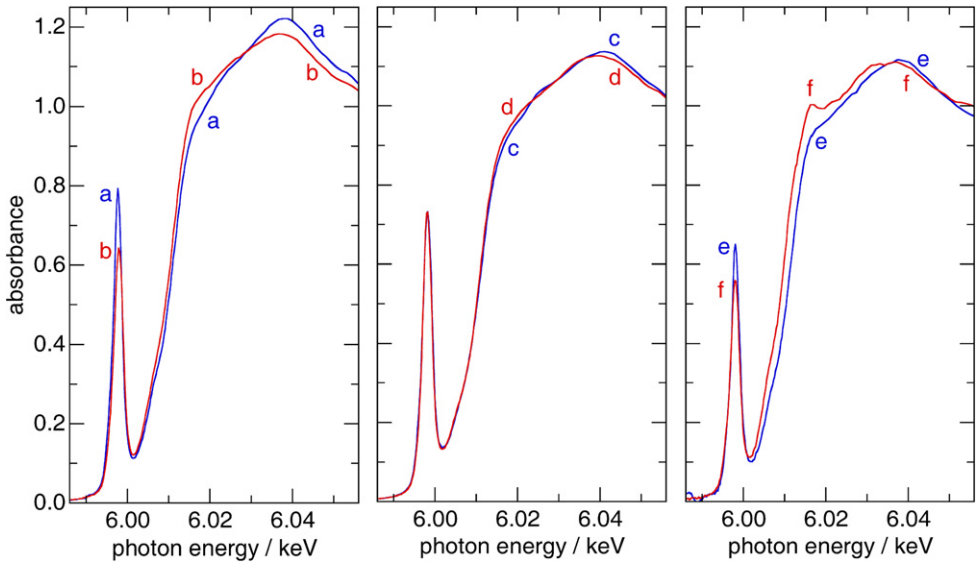

Fig. 6. Comparison of normalized XANES spectra for two CrO_2Cl_2-modified silicas (left panel): (a) S952-200 and (b) S952-800; both recorded after heating *in vacuo* at 200 °C; as well as for two molecular silylchromate diesters (middle panel): (c) acyclic $CrO_2(OSiPh_3)_2$ and (d) cyclic $[CrO_2\{(OSiPh_2)_2O\}]_2$; and for a standard Phillips catalyst Cr/SiO_2 calcined at 800 °C (right panel), with (e) 0.66 wt% Cr and (f) 1.0 wt% Cr.

Since both model compounds have the same first-coordination sphere, this comparison suggests that the differences arise from the XANES contributions of Si next-nearest neighbors.

Finally, the XANES of the Phillips catalyst was investigated. In this case, it is necessary to correctly attribute those features of the XANES that are due to α-Cr_2O_3, since it is commonly present when the catalyst is prepared by wet impregnation with a high Cr loading, or when it is heated in an inert/reducing atmosphere prior to calcination under O_2 [48]. The XANES of two catalysts containing (i) 0.66 wt% Cr, heated to 800 °C under flowing O_2, and (ii) 1.0 wt% Cr, heated to 800 °C prior to the addition of O_2, are shown in Figs. 6e and 6f. The former contains no characteristics of α-Cr_2O_3, according to linear combination XANES analysis (using the spectra of the molecular silylchromate diesters $CrO_2(OSiPh_3)_2$ and $[CrO_2\{(OSiPh_2)_2O\}]_2$ to represent the contributions of the chromate sites). Furthermore, the intensity of the pre-edge peak (0.65) is similar to that of the chromate sites (0.64) derived from chromyl chloride-modified S952-800, Fig. 6b. However, the catalyst with the higher Cr content shows characteristic peaks for octahedral Cr in α-Cr_2O_3 at 6.016 and 6.032 keV, as well as reduced intensity (0.56) of the pre-edge peak caused by the coexistence of both octahedral Cr(III) and pseudo-tetrahedral Cr(VI) environments. The same linear combination analysis, applied to the chromates formed by heating grafted $\equiv SiOCrO_2Cl$ sites, gave no evidence for α-Cr_2O_3, even on S952-200 with a Cr loading of 1.5 wt%.

3.6. EXAFS analysis

The Fourier-transformed k^3-weighted EXAFS of each of the CrO_2Cl_2-modified silicas prior to heating consist of two peaks at ca. 1.2 and 1.8 Å in R-space. They are associated with backscattering from oxygen and chlorine, respectively [11]. Treating each of these materials at 200 °C *in vacuo* causes the peak at ca. 1.8 Å in R-space to disappear, Figs. 7a and 7b. This is consistent with elimination of chloride from the coordination sphere of Cr and also, for S952-200 and S952-450, from the solid (as shown by elemental analysis, described above). In the spectrum of CrO_2Cl_2-modified S952-200, a new peak appears at 1.5 Å, Fig. 7a. This feature is considerably weaker in the EXAFS of CrO_2Cl_2-modified S952-450 (Fig. S1), and is not visible at all in the spectrum of CrO_2Cl_2-modified S952-800, Fig. 7b. The EXAFS of the Phillips catalyst (0.66 wt% Cr/SiO_2, calcined at 800 °C) consists of a peak at 1.2 Å and a weak feature at 1.7 Å, Fig. 7c.

The Fourier-transformed k^3-weighted EXAFS of two molecular silylchromate diesters were recorded for comparison, Fig. 7d. Although each compound has the same first coordination sphere at Cr, their EXAFS is quite different. The spectrum of acyclic $CrO_2(OSiPh_3)_2$ consists of two well-resolved peaks at 1.1 and 1.5 Å, while the spectrum of cyclic $[CrO_2\{(OSiPh_2)_2O\}]_2$ shows only a single broad peak, centered at 1.2 Å.

The EXAFS curvefit for $CrO_2(OSiPh_3)_2$, using a simple silylchromate diester model and single-scattering paths in the first coordination sphere only (Cr=O, $N = 2$; Cr–O, $N = 2$), returned distances (1.60, 1.77 Å) in agreement with the average values for the two types of bonds in the reported crystal structure [49], Table S1. Both Cr=O distances and Cr–O distances are inequivalent in the solid-state, although the EXAFS data range for the first coordination sphere ($3.0 \leqslant k \leqslant 15.0$ Å^{-1}; $0.8 \leqslant R \leqslant 1.8$ Å) does not permit refinement to four independent paths, according to the Nyquist theorem ($N_{idp} = 7.6$). Weak features between 2.5 and 3.5 Å in R-space may arise from Cr–Si single-scattering paths and/or various multiple-scattering events involving the oxo ligands. All are predicted by FEFF to have comparable intensities, complicating the analysis of this region [50]. Since the single-scattering paths of the first-coordination sphere are well-separated from weak features at higher R, further analysis of the latter was not attempted. Compared to $CrO_2(OSiPh_3)_2$, the cyclic diester $[CrO_2\{(OSiPh_2)_2O\}]_2$ gives EXAFS with a shorter k-range of usable data (Figs. S2 and S3 and Table S2), resulting in lower resolution for both the short and long Cr–O paths. However, the EXAFS fit gives bond distances that are the same as those for the acyclic diester (1.60, 1.76 Å), within the accepted error of the EXAFS techniques (±0.02 Å).

After heating at 200 °C, CrO_2Cl_2-modified S952-200 gives EXAFS most closely resembling that of acyclic $CrO_2(OSiPh_3)_2$, with two clearly resolved peaks at low R. The curvefit to the single-site chromate diester model (Cr=O, $N = 2$; Cr–O, $N = 2$) is shown in Figs. 8a and 8b, with fit parameters given in Table 3. The bond lengths for the Cr=O and Cr–O paths, 1.60 and 1.78 Å, respectively, are the same as those of the model compound. The Debye–Waller factors are small (<0.003 Å^2), consistent with uniform chromate sites of C_{2v} symmetry. The EXAFS of the chromate sites made by heating CrO_2Cl_2-modified S952-800, consisting of a single broad peak in the FT magnitude, resembles that of the cyclic model com-

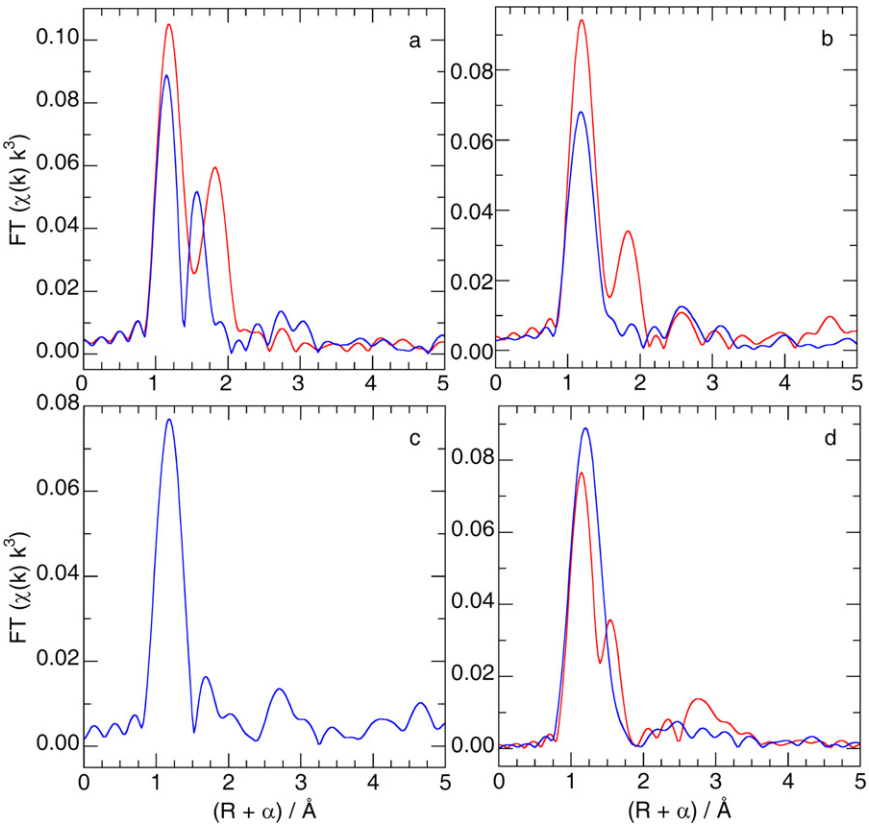

Fig. 7. Comparisons of Fourier-transformed k^3-weighted EXAFS magnitudes, for (a) CrO_2Cl_2-modified S952-200; and (b) CrO_2Cl_2-modified S952-800; each before (red) and after (blue) heating *in vacuo* at 200 °C; (c) for CrO_3 on Sylopol 952 (Phillips catalyst, 0.66 wt% Cr), after calcination at 800 °C; and (d) for the molecular silylchromate diesters $[CrO_2\{(OSiPh_2)_2O\}]_2$ (blue) and $CrO_2(OSiPh_3)_2$ (red). (For interpretation of the references to color in this figure legend, the reader is referred to the web version of this article.)

pound $[CrO_2\{(OSiPh_2)_2O\}]_2$. The spectrum was first analyzed with a tetrahedral chromate model (CrO_4^{2-}) involving a single Cr–O path ($N = 4$). The fit returned a bond length of 1.65 Å with an unacceptably large Debye–Waller factor, 0.016 $Å^2$, and a large residual (39.1). The curvefit obtained with two single-scattering paths (Cr=O, $N = 2$; Cr–O, $N = 2$) is shown in Figs. 8c and 8d. Both fitted bond lengths are the same as those obtained from S952-200, Table 3, however, the Debye–Waller factors for both paths are larger. This may reflect a symmetry lower than C_{2v} (as suggested by the XANES analysis), or less uniformity in the chromate sites present on S952-800. However, the data range does not permit the inclusion of more independent paths. The curvefit to the EXAFS of the Phillips catalyst, Fig. S4, is similar to those of the silica-supported chromates modified with CrO_2Cl_2, Table 3, but with even larger Debye–Waller factors, suggesting even greater heterogeneity of the chromate sites.

3.7. XANES simulation

According to the EXAFS, all of the chromate structures described here, including the molecular compounds and the modified silicas, possess similar bond distances in their first coordination spheres, giving little insight into the distinguishing features of those sites that are capable of initiating ethylene polymerization versus those that do not. It is therefore of interest to probe interactions beyond the first coordination sphere, although the EXAFS is not much help in this regard, as a result of destructive interference between single- and multiple-scattering paths (see above). However, XANES is sensitive to the relative positions of atoms both in and beyond the first coordination sphere because of multiple scattering. These contributions were simulated for the relatively unstrained 8-membered chromasiloxane ring **II**, and the more strained 6-membered chromasiloxane ring **V**.

The simulated XANES spectra are compared in Fig. 9. In all spectra, the sharp, intense pre-edge feature typical of pseudo-tetrahedral sites is reproduced. Transformation of the simple monochlorosilylchromate monoester $CrO_2Cl(OSiH_2OH)$ to the silylchromate diester **II** is characterized by disappearance of the shoulder on the absorption edge at ca. 5 eV, Figs. 9a and 9b. The same behavior was seen in the experimental XANES for all three types of CrO_2Cl_2-modified silicas (Fig. 5). This feature was previously correlated with chlorine density-of-states, and its disappearance therefore confirms loss of the chloride ligand from the coordination sphere of Cr for all silicas upon heating at 200 °C. The simulated XANES intensity also increases at ca. 10 and 30 eV (relative photon energy), but decreases at ca. 20 eV.

XANES simulation of the smaller chromasiloxane ring **V** shows a lower intensity for the pre-edge peak, a higher intensity prior to the first maximum (ca. 12 eV), and a lower intensity at the first maximum (ca. 20 eV) compared to the simulated XANES of **II**, Figs. 9b and 9c. These trends are consistent with differences observed in the experimental spectra when the silica pretreatment temperature was increased from 200 to 800 °C (Figs. 6a and 6b). The calculated densities of states for the two model chromasiloxane rings show that changes in features superimposed on the edge arise from changes in the hybridization and mixing of the Cr-4*p* states, Fig. 10, since the relative intensities of the contributions at 10 and 20 eV depend on the chromasiloxane ring size. In particular, the intensity of the Si-3*d* contribution is higher at 20 eV for **II**, but higher at 10 eV for **V** in parallel with changes in the calculated and experimental XANES.

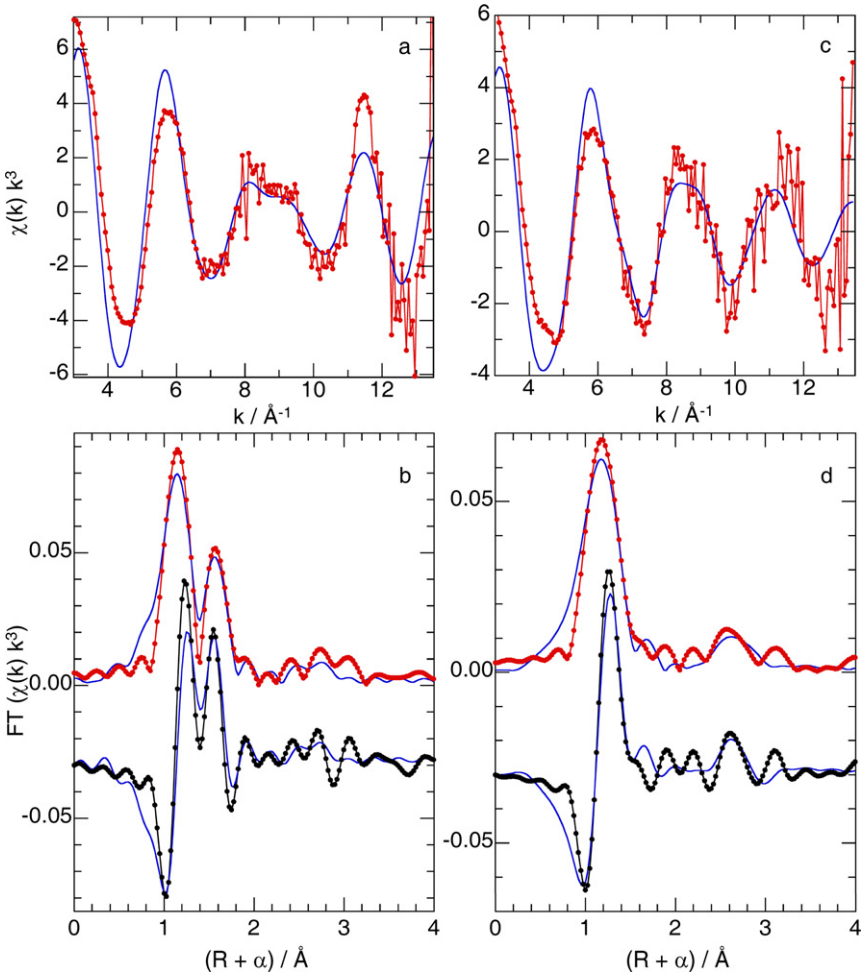

Fig. 8. Single-scattering refinements of the $(\equiv SiO)_2CrO_2$ model to EXAFS of CrO_2Cl_2 grafted on Sylopol 952 pretreated at 200 °C (a, b) and 800 °C (c, d), after treatment *in vacuo* at 200 °C. Top: data (red points) and fit (blue line) in *k*-space. Bottom: FT magnitude (red points) and imaginary component (black points) and curvefits (blue) fits in *R*-space. (For interpretation of the references to color in this figure legend, the reader is referred to the web version of this article.)

Table 3
Curvefit parameters for the single-scattering refinements[a] of the $(\equiv SiO)_2CrO_2$ model to EXAFS of materials made by grafting CrO_2Cl_2 onto Sylopol 952, followed by heating at 200 °C *in vacuo*, and to EXAFS of the Phillips catalyst.

Support	Path	N[b]	R (Å)	σ^2 (Å^2)	ΔE_0 (eV)
S952-200[c]	Cr=O	2	1.60	0.0023	−0.8
	Cr–O	2	1.78	0.0023	
S952-800[d]	Cr=O	2	1.60	0.0053	−1.4
	Cr–O	2	1.77	0.010	
Phillips catalyst[e]	Cr=O	2	1.61	0.0055	0.6
	Cr–O	2	1.79	0.014	

[a] Errors for first-shell scattering fits calculated against EXAFS data, in the absence of systematic fitting errors, are generally accepted to be as follows: bond lengths ± 0.02 Å, σ^2 ± 20%, ΔE_0 ± 20% [61].

[b] Coordination numbers were fixed at integer values.

[c] *k*-range 3.0–13.5 Å^{-1}; residual = 24.7; $S_0^2 = 0.91$.

[d] *k*-range 3.0–13.5 Å^{-1}; residual = 20.8; $S_0^2 = 0.93$.

[e] Cr/SiO_2 (0.66 wt% Cr), calcined at 800 °C; *k*-range 3.0–13.0 Å^{-1}; residual = 21.7; $S_0^2 = 0.93$.

4. Discussion

Direct formation of chloride-free silylchromate diesters during the deposition of CrO_2Cl_2 onto various silicas has been reported for grafting conducted at elevated temperatures (⩾170 °C) [12,13,51,52]. However, we proposed that the first-formed $\equiv SiOCrO_2Cl$ sites evolve to chloride-free chromate diester sites by subsequent condensation reactions [11], Eq. (6).

$$\equiv SiOCrO_2Cl\ldots HOSi\equiv \rightarrow (\equiv SiO)_2CrO_2 + HCl \quad (6)$$

Our results confirm that, upon mild heating of CrO_2Cl_2-modified silicas *in vacuo* at 200 °C, $\equiv SiOCrO_2Cl$ is converted quantitatively to an anchored chromate site, $(\equiv SiO)_2CrO_2$. This transformation does not occur spontaneously at room temperature, consistent with our calculations that predict the condensation of monochlorosilylchromate monoesters with an adjacent hydroxyl group to be endothermic. Experimentally, we observe an increase in intensity of an IR band at 905 cm^{-1} assigned to CrO–Si vibrations, and slight changes in the frequencies of the $\nu(CrO_2)$ overtones in the directions predicted for the calculated vibrational frequencies of model clusters. The chloride-to-ester transformation is further demonstrated by the disappearance of features in both the EXAFS and XANES attributed to the presence of Cr–Cl bonds [11].

The expected chloride loss from these materials upon chromate formation was indeed observed for both CrO_2Cl_2-modified S952-200 and S952-450. Decreases in Cl/Cr ratios reported upon heating CrO_2Cl_2-modified silicas under N_2 at 400 °C were also attributed to the transformation of $\equiv SiOCrO_2Cl$ sites to $(\equiv SiO)_2CrO_2$ [13]. However, the chloride content of CrO_2Cl_2-modified S952-800 declines only slightly upon heating to 200 °C. This suggests that most chromate sites on the highly dehydroxylated silica are formed by a mechanism other than reaction with residual surface hydroxyls.

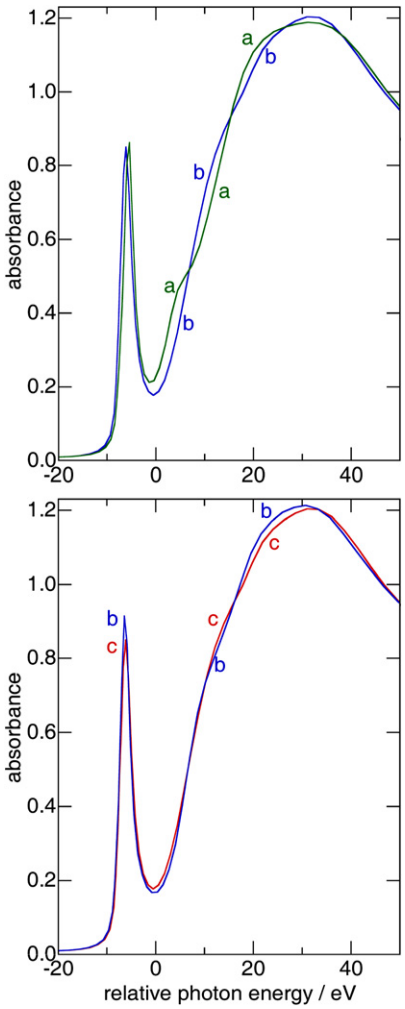

Fig. 9. Comparison of simulated XANES spectra for (a) a chlorosilylchromate monoester, $CrO_2Cl(OSiH_2OH)$ (green); (b) chromate in an 8-membered chromasiloxane ring **II** (blue); and (c) chromate in a 6-membered chromasiloxane ring **V** (red). (For interpretation of the references to color in this figure legend, the reader is referred to the web version of this article.)

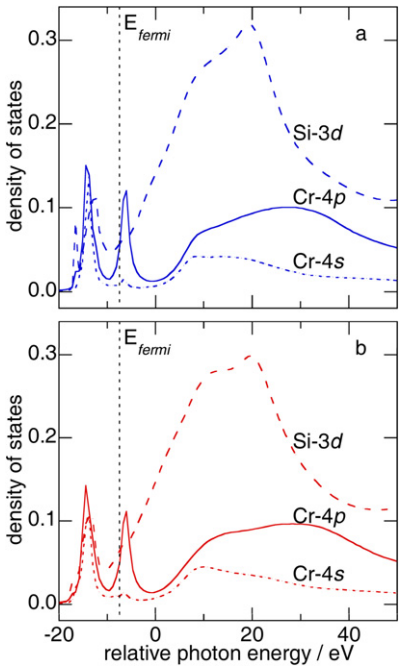

Fig. 10. Calculated (FEFF 8.2) density-of-states for two model chromates in chromasiloxane rings: (a) 8-membered ring **II** (blue); and (b) 6-membered ring **V** (red). (For interpretation of the references to color in this figure legend, the reader is referred to the web version of this article.)

This reaction is suggested to be transfer of chloride from Cr to Si, Scheme 4.

The positions of the CrO_2 stretching modes appear to be insensitive to structural differences between silylchromate diesters that lead to active and inactive sites. This suggests that their distinguishing characteristics may be more directly related to the features of the chromasiloxane rings rather than the CrO_2 fragments. X-ray absorption spectroscopy has the potential to provide more detailed local information, but its application to Phillips catalysts has mostly involved materials that were not prepared under conditions representative of the commercial catalyst ($\leqslant$1 wt% Cr; calcination temperature $\geqslant$700 °C, and strict exclusion of moisture after activation to prevent the hydrolysis of silyl ester bonds). For example, the EXAFS of samples calcined at low temperatures, or exposed to air [53,54], is of little relevance because these materials are inactive. High Cr loadings [48,53,55] are problematic because the EXAFS contains contributions from multiple Cr sites. For example, the X-ray absorption spectrum of a 4 wt% Cr/SiO_2 catalyst (1.2 Cr/nm^2) activated at 500 °C had a very short k-range of usable data (to 7 $Å^{-1}$), attributed to destructive interference from several components including a significant amount of Cr_2O_3; no curve-fitting was attempted [48]. The most informative XAS study of an anhydrous silica-supported chromate with low Cr loading was reported for a xerogel containing 0.5 mol% Cr, calcined at 500 °C [41]. Two peaks were resolved in the R-space EXAFS, corresponding to bond distances of 1.60 and 1.80 Å for a diester model with Cr=O ($N = 2$) and Cr–OSi ($N = 2$) paths, respectively. However, ethylene polymerization with this material was not attempted.

Our results demonstrate that while silylchromate diesters present on CrO_2Cl_2-modified and heated silicas pretreated at all three temperatures (200, 450 and 800 °C) are more uniform than those prepared by aqueous methods, they are neither structurally equivalent nor equally reactive toward ethylene. The differences may be attributed to Cr–support interactions. Since variations in the XANES of the supported chromates on S952-200 and S952-800 are reproduced in the simulated spectra for 8- and 6-membered chromasiloxane rings, we suggest that the former are created exclusively on the silica pretreated at low temperature, while the latter are present in increasing amounts on silicas pretreated at higher temperatures. The decreasing intensity of the pre-edge peak with increasing silica dehydroxylation temperature is attributed to distortion from tetrahedral symmetry as the fraction of strained rings increases, since O–Cr–O angles in the 8- and 6-membered rings **II** and **V** are 109 and 105°, respectively. Differences in the post-edge XANES are consistent with the changes in hybridization and mixing of the Cr 4p-orbitals with the Cr 4s- and Si 3d-orbitals in the two chromasiloxane rings.

Well-defined molecular chromium complexes that model Cr–support interactions have thus far failed to reproduce the initiation of polymerization exhibited by the Phillips catalyst; in particular, polymerization of ethylene by a soluble silylchromate diester has not been observed. For example, $CrO_2(OSiPh_3)_2$ is inactive toward ethylene in the absence of either silica or an alkylaluminum activator [56]. Its failure to activate was attributed to electron donation from the triphenylsilanolate ligands. However, the less electron-rich chromate diester $[(c\text{-}C_6H_{11})_7Si_7O_{11}(OSiMe_3)CrO_2]$ containing chromate bound to an incompletely condensed silsesquioxane cube does not polymerize ethylene spontaneously either [32]. The chromate in that compound was described as being attached to "vicinal" silanol groups, although the silanolates are not, in fact, dis-

posed vicinally (i.e., located on silicon atoms separated by a single bridging oxygen). The anchored chromate is actually contained in an 8-membered chromasiloxane ring. The reaction of CrO_3 with tetraphenyldisiloxanediol in the presence of molecular sieves fails to produce $[CrO_2\{(OSiPh_2)_2O\}]$, but gives instead the 12-membered ring compound $[CrO_2\{(OSiPh_2)_2O\}]_2$ [26], presumably to avoid the ring strain of the 6-membered chromasiloxane ring.

Residual silanols have been suggested to play a role in the polymerization initiation process, either as a source of hydrogen involved in forming alkylchromium active sites [57,58], or as poisons of those sites [5,59]. The latter role is generally invoked to explain the increase in activity with increasing calcination temperature. However, the silanol population may be merely a proxy for surface strain. As described above, it is notable that solutions of molecular silylchromate diesters, containing no free silanols, fail to initiate ethylene polymerization spontaneously (i.e., to reproduce the behavior of the Phillips catalyst). Increased strain was suggested to explain the easier reducibility of Cr(VI) on Phillips catalysts calcined at higher temperatures [1], although the nature of this "strain" has not been elucidated. The greater *average* distance between surface hydroxyls used to anchor chromates to the silica surface as calcination temperature increases was suggested to create strain by causing an increase in the O–Cr–O angle of the chromasiloxane rings [60], however, a computational study showed that the opposite is true: higher ring strain is associated with the smaller O–Cr–O angles found in smaller rings [37]. Such rings are formed when CrO_2Cl_2 reacts with the hydroxyls that persist on silicas calcined at higher temperatures, since vicinal silanols resist condensation even at 800 °C [34]. Consistent with this hypothesis, the activation barriers for ethylene insertion and β-H elimination in chromacycloalkane rings (modeling steps in Phillips-catalyzed ethylene oligomerization) decreased dramatically with increased chromasiloxane ring strain [37].

5. Conclusions

Model Phillips catalysts containing uniform chromate sites anchored onto silica via an anhydrous grafting technique can be described as CrO_2 fragments embedded in chromasiloxane rings. The ring strain is a function of ring size. IR, XANES and EXAFS are consistent with strained rings (containing 6 atoms, CrOSiOSiO) being more abundant on silicas pretreated at higher temperatures. These catalysts also show higher ethylene polymerization activities, suggesting that ring strain is also associated with a critical step in the initiation process, and perhaps also in chain-propagating reactions. The well-defined chromate sites on silica pretreated at 200 °C fail to activate, presumably because the chromasiloxane rings are exclusively unstrained (containing at least 8 atoms, CrOSiOSiOSiO).

Acknowledgments

The authors thank Prof. Baron Peters for helpful discussions. This work was supported by the National Science Foundation under Grant No. 500489. Portions of this research were carried out at the Stanford Synchrotron Radiation Lightsource, a national user facility operated by Stanford University on behalf of the U.S. Department of Energy, Office of Basic Energy Sciences.

Supporting information

The online version of this article contains additional supplementary material (optimized energies of model compounds with Cartesian coordinates; additional EXAFS fits and parameters).

Please visit DOI: 10.1016/j.jcat.2008.11.024.

References

[1] M.P. McDaniel, in: G. Ertl, H. Knözinger, F. Schüth, J. Weitkamp (Eds.), Handbook of Heterogeneous Catalysis, Wiley–VCH, Weinheim, 2008, p. 3733.
[2] B.M. Weckhuysen, I.E. Wachs, R.A. Schoonheydt, Chem. Rev. 96 (1996) 3327.
[3] E.L. Lee, I.E. Wachs, J. Phys. Chem. C 111 (2007) 14410.
[4] M.P. McDaniel, Adv. Catal. 33 (1985) 47.
[5] M.P. McDaniel, M.B. Welch, J. Catal. 82 (1983) 98.
[6] E.M.E. van Kimmenade, A.E.T. Kuiper, Y. Tamminga, P.C. Thüne, J.W. Niemantsverdriet, J. Catal. 223 (2004) 134.
[7] G. Agostini, E. Groppo, S. Bordiga, A. Zecchina, C. Prestipino, F. D'Acapito, E. van Kimmenade, P.C. Thüne, J.W. Niemantsverdriet, C. Lamberti, J. Phys. Chem. C 111 (2007) 16437.
[8] P.C. Thüne, R. Linke, W.J.H. van Gennip, A.M. de Jong, J.W. Niemantsverdriet, J. Phys. Chem. B 105 (2001) 3073.
[9] C.N. Nenu, E. Groppo, C. Lamberti, A.M. Beale, T. Visser, A. Zecchina, B.M. Weckhuysen, Angew. Chem. Int. Ed. 46 (2007) 1465.
[10] C.N. Nenu, J.N. van Lingen, F.M.F. de Groot, D.C. Koningsberger, B.M. Weckhuysen, Chem. Eur. J. 12 (2006) 4756.
[11] C.A. Demmelmaier, R.E. White, J.A. van Bokhoven, S.L. Scott, J. Phys. Chem. C 112 (2008) 6439.
[12] M. Nishimura, J.M. Thomas, Catal. Lett. 19 (1993) 33.
[13] M.P. McDaniel, J. Catal. 76 (1982) 17.
[14] M. Nishimura, J.M. Thomas, Catal. Lett. 21 (1993) 149.
[15] E. Groppo, C. Lamberti, S. Bordiga, G. Spoto, A. Zecchina, Chem. Rev. 105 (2005) 115.
[16] Y.V. Plyuto, Y.I. Gorlov, A.A. Chuiko, Teor. Eksp. Khim. 19 (1983) 494.
[17] N.V. Borisenko, P.A. Mutovkin, Y.V. Plyuto, Kinet. Catal. 38 (1997) 103.
[18] M. Alam, M.A. Henderson, P.D. Kaviratna, G.S. Herman, C.H.F. Peden, J. Phys. Chem. B 102 (1998) 111.
[19] A.A. Malygin, Zh. Obshch. Khim. 49 (1979) 1936.
[20] A.A. Malygin, A.A. Malkov, S.D. Dubrovenskii, in: A. Dabrowski, V.A. Tertykh (Eds.), Adsorption on New and Modified Inorganic Sorbents, Elsevier Science, 1996, p. 213.
[21] D. Damyanov, L. Vlaev, Bull. Chem. Soc. Jpn. 56 (1983) 1841.
[22] B.A. Morrow, I.A. Cody, J. Phys. Chem. 80 (1976) 1998.
[23] T.A. Michalske, B.C. Bunker, J. Appl. Phys. 56 (1984) 2686.
[24] B.C. Bunker, D.M. Haaland, T.A. Michalske, W.L. Smith, Surf. Sci. 222 (1989) 95.
[25] P.C. Thüne, C.P.J. Verhagen, M.J.G. van den Boer, J.W. Niemantsverdriet, J. Phys. Chem. 101 (1997) 8559.
[26] H.C. Abbenhuis, M.L. Vorstenbosch, R.A. van Santen, W.J.J. Smeets, A.L. Spek, Inorg. Chem. 36 (1997) 6431.
[27] L.M. Baker, W.L. Carrick, J. Org. Chem. (1970) 774.
[28] I. Arcon, B. Mirtic, A. Kodre, J. Am. Ceram. Soc. 81 (1998) 222.
[29] M. Newville, The XAFS Model Compound Library; http://cars9.uchicago.edu/~newville/ModelLib/.
[30] A.L. Ankudinov, C. Bouldin, J.J. Rehr, J. Sims, H. Hung, Phys. Rev. B 65 (2002) 104.
[31] D.R. Tallant, B.C. Bunker, C.J. Brinker, C.A. Balfe, Mater. Res. Soc. Symp. Proc. 73 (1986) 261.
[32] F.J. Feher, R.L. Blanski, J. Chem. Soc. Chem. Commun. (1990) 1614.
[33] F.L. Galeener, in: P.H. Gaskell, J.M. Parker, E.K. Davis (Eds.), The Structure of Non-Crystalline Materials, Taylor and Francis, London, 1982, p. 337.
[34] Z.A. Taha, E.W. Deguns, S. Chattopadhyay, S.L. Scott, Organometallics 25 (2006) 1891.
[35] B.C. Bunker, D.M. Haaland, K.J. Ward, T.A. Michalske, W.L. Smith, J.S. Binkley, C.F. Melius, C.A. Balfe, Surf. Sci. 210 (1989) 406.
[36] T.J. Dines, S. Inglis, Phys. Chem. Chem. Phys. 5 (2003) 1320.
[37] Ø. Espelid, K.J. Børve, J. Catal. 195 (2000) 125.
[38] B.A. Morrow, I.A. Cody, J. Phys. Chem. 79 (1975) 761.
[39] W.E. Hobbs, J. Chem. Phys. 28 (1958) 1220.
[40] E.L. Lee, I.E. Wachs, J. Phys. Chem. C 112 (2008) 6487.
[41] C. Moisii, E.W. Deguns, A. Lita, S.D. Callahan, L.J. van de Burgt, D. Magana, A.E. Stiegman, Chem. Mater. 18 (2006) 3965.
[42] M.A. Vuurman, I.E. Wachs, D.J. Stufkens, A. Oskam, J. Mol. Catal. 80 (1993) 209.
[43] I. Arcon, A. Kodre, in: Materials Characterization by X-ray Absorption Spectroscopy (EXAFS, XANES), Proceedings of the 36th International Conference on Microelectronics, Devices and Materials, Postojna, Slovenia, 2000, p. 191.
[44] C. Pak, G.L. Haller, Micropor. Mesopor. Mater. 48 (2001) 165.
[45] Y. Wang, Y. Ohishi, T. Shishido, Q. Zhang, W. Yang, Q. Guo, H. Wan, K. Takehira, J. Catal. 220 (2003) 347.
[46] L.A. Grunes, Phys. Rev. B 27 (1983) 2111.
[47] J. Wong, F.W. Lytle, R.P. Messmer, D.H. Maylotte, Phys. Rev. B 30 (1984) 5596.
[48] E. Groppo, C. Prestipino, F. Cesano, F. Bonino, S. Bordiga, C. Lamberti, P.C. Thüne, J.W. Niemantsverdriet, A. Zecchina, J. Catal. 230 (2005) 98.
[49] B. Stensland, P. Kierkegaard, Acta Chem. Scand. 24 (1970) 211.
[50] K.I. Pandya, Phys. Rev. B 50 (1994) 15509.
[51] A.N. Volkova, V.M. Smirnov, V.B. Aleskovskii, A.A. Malygin, S.I. Koltsov, Zh. Obshch. Khim. 42 (1972) 1431.
[52] D. Mehandjiev, S. Angelov, D. Damyanov, Stud. Surf. Sci. Catal. 3 (1979) 605.
[53] A. Ellison, G. Diakun, P. Worthington, J. Mol. Catal. 46 (1988) 131.

[54] F.G. Requejo, J.M. Ramallo-López, R. Rosas-Salas, J.M. Domínguez, J.A. Rodriguez, J.-Y. Kim, R. Quijada, Catal. Today 107–108 (2005) 750.
[55] B.M. Weckhuysen, R.A. Schoonheydt, J.-M. Jehng, I.E. Wachs, S.J. Cho, R. Ryoo, S. Kijistra, E. Poels, J. Chem. Soc. Faraday Trans. 91 (1995) 3245.
[56] W.L. Carrick, R.J. Turbett, F.J. Karol, G.L. Karapinka, A.S. Fox, R.N. Johnson, J. Polym. Sci. Part A Polym. Chem. 10 (1972) 2609.
[57] C. Groenveld, P.P.M.M. Wittgen, H.P.M. Swinnen, A. Wernsen, G.C.A. Schuit, J. Catal. 83 (1983) 346.
[58] W.K. Jozwiak, I.G. Dalla Lana, R. Fiederow, J. Catal. 154 (1995) 329.
[59] H.L. Krauss, Z. Anorg. Allg. Chem. 414 (1975) 97.
[60] B. Liu, F. Yuwei, M. Terano, J. Mol. Catal. A Chem. 219 (2004) 165.
[61] M. Vaarkamp, Catal. Today 39 (1998) 271.